Journal of Power Sources 186 (2009) 349–352

Contents lists available at ScienceDirect

Journal of Power Sources

journal homepage: www.elsevier.com/locate/jpowsour

Short communication

The effect of homovalent A-site substitutions on the ionic conductivity of pyrochlore-type $Gd_2Zr_2O_7$

J.A. Díaz-Guillén [a], A.F. Fuentes [a,*], M.R. Díaz-Guillén [a], J.M. Almanza [a], J. Santamaría [b], C. León [b]

[a] Cinvestav-Saltillo, Apartado Postal 663, 25000 Saltillo, Coahuila, Mexico
[b] GFMC, Departamento de Física Aplicada III, Facultad de Física, Universidad Complutense de Madrid, 28040 Madrid, Spain

ARTICLE INFO

Article history:
Received 26 August 2008
Received in revised form
26 September 2008
Accepted 30 September 2008
Available online 10 October 2008

Keywords:
Pyrochlores
$Gd_2Zr_2O_7$
Ionic conductivity
Anion deficient fluorites

ABSTRACT

We evaluate in this work the effect of Gd substitution on the dc activation energy, E_{dc}, and ionic conductivity of the pyrochlore-type gadolinium zirconate, P-$Gd_2Zr_2O_7$. Several compositions with the general formulae $Gd_{2-y}Ln_yZr_2O_7$ (Ln = Er^{3+}, Y^{3+}, Dy^{3+}, Sm^{3+}, Nd^{3+} and La^{3+}) were prepared by mechanically milling and firing stoichiometric mixtures of the corresponding elemental oxides and their electrical properties analyzed as a function of frequency and temperature by using impedance spectroscopy. Whereas Gd substitution in P-$Gd_2Zr_2O_7$ by smaller lanthanides induces a pyrochlore to fluorite phase transition, using larger dopant cations yields partially disordered pyrochlores. Despite of higher structural disorder, ionic conductivity values measured for the fluorite-type materials are lower than those observed for pyrochlores whereas activation energies for oxygen migration in the series decrease monotonically as the average size of the A cation increases.

1. Introduction

Solid oxide fuel cells (SOFCs) are highly efficient and environmentally friendly energy conversion devices with a large variety of potential applications. Current SOFCs technology is based on the $La_xSr_{1-x}MnO_3$ (LSM) cathode, the yttria stabilized zirconia (YSZ) electrolyte and Ni-YSZ cermet anode. As cells are operated at high temperatures under either oxidising or reducing atmospheres over a long period of time, different materials-related problems associated with such aggressive environments, limit their long-term stability. Thus, solid state reactions taking place at the cathode/electrolyte interface cause the formation of insulating phases such as $La_2Zr_2O_7$ and $SrZrO_3$, both having a detrimental effect on cell performance. A possibility to overcome this problem would be using the LSM cathode but with a different and compatible electrolyte. In this context, oxides $A_2B_2O(1)_6O(2)$ with the pyrochlore-type crystal structure, represent an interesting group of solid oxide ion conducting materials because of their high compositional diversity, structural flexibility and intrinsic concentration of oxygen vacancies [1–3]. The *ideal* cubic pyrochlore structure might be derived from that of an anion deficient fluorite by doubling the unit cell, removing one out of every eight anions and placing cations and anions in four fully occupied and non-equivalent sites: 16*c* and 16*d* for cations (Wyckoff notation) and 48*f* and 8*a* for anions (see [4] for a detailed description of the pyrochlore crystal structure). There is a third position in the unit cell available for anions, 8*b*, which is systematically empty in *ideal* (*ordered*) and thus, non-conductive pyrochlores but partially occupied in *defect* (*disordered*) anion conducting materials. According to several computational calculations, the most stable intrinsic anion defect in pyrochlores is an oxygen Frenkel pair consisting of a vacant 48*f* position and an interstitial oxygen ion located at the 8*b* site [5–8]. The energy needed to create this defect might be significantly lowered by disordering the cation substructure, that is, by inducing homogeneous cation environments of the oxygen atoms [1]. Thus, partially disordered phases are better ionic conductors than the fully disordered fluorite materials of the same composition because of smaller activation energies for migration; e.g., the E_{dc} is significantly lower in the *defect* pyrochlore-type gadolinium zirconate (P-$Gd_2Zr_2O_7$) than in its fully disordered analogue, the fluorite-type F-$Gd_2Zr_2O_7$ [9]. Interestingly, structural disorder in this type of compounds is to a great extent linked to the A to B size mismatch (the R_A/R_B size ratio) and thus, materials showing different degrees of disorder are possible by using the appropriate cation combinations. Therefore, pyrochlores are an excellent model system to analyze the influence of structural disorder in ion mobility.

Although there is a growing interest in this type of materials, the understanding of the effect of A and/or B substitutions on oxide ion migration is inadequate at this point. Atomic scale computing simulations have predicted the activation energy for oxygen

* Corresponding author. ARAID-Instituto de Ciencia de Materiales de Aragon, C.S.I.C.-Universidad de Zaragoza, 50009-Zaragoza, Spain. Tel.: +52 8444389600; fax: +52 8444389610.
E-mail address: fuentesaf@live.com (A.F. Fuentes).

0378-7753/$ – see front matter © 2008 Elsevier B.V. All rights reserved.
doi:10.1016/j.jpowsour.2008.09.106

migration in A^{3+}/B^{4+} pyrochlores to be strongly dependent on the average B-site cation size and give a secondary role to the A cation [5]. However experimental data do not confirm clearly these predictions. Particularly, the effect of A-site homovalent substitutions on the activation energy and conductivity of pyrochlores, has not been completely understood and studies have mostly focused in the $A_2(B_{1-y}B'_y)_2O_7$ systems, with two tetravalent cations (B, B′ = Sn^{4+}, Ti^{4+}, Zr^{4+}) simultaneously occupying the hexa-coordinated 16*d* site and a single trivalent cation (A = Y^{3+} or Ln^{3+}) on the octa-coordinated 16*c* site [1]. The aim of the present contribution is to study the role played by the average A cation size on the electrical properties of P-$Gd_2Zr_2O_7$, a well-known high-temperature solid oxide ion conductor. As the size of the B-cation would be constant when replacing Gd by another homovalent lanthanide, electrical properties would be mostly affected by the average A cation size and its influence on structural ordering/disordering. As we have already shown [10,11], La incorporation into $Gd_2Zr_2O_7$ decreases the dc activation energy and even increases its ionic conductivity at low temperatures. We will now extend this study to some other trivalent lanthanides (Er, Y, Dy, Nd and Sm) and compare these results with those previously obtained with La.

2. Experimental

A set of $Gd_{2-y}Ln_yZr_2O_7$ materials with Ln = Er^{3+}, Y^{3+}, Dy^{3+}, Sm^{3+}, Nd^{3+} and La^{3+} (see Table 1 for a complete list) were prepared by mechanically milling stoichiometric mixtures of high purity elemental oxides Gd_2O_3, ZrO_2 and Ln_2O_3 (Ln = La, Nd, Sm, Dy, Y, Er), as described in previous works carried out in this group (see for example [12,13]). Powders were mixed and dry milled together in a planetary ball mill by using stabilized zirconia vials and balls and a moderate rotating disc speed (350 rpm). Phase evolution of milled samples was followed by using X-ray power diffraction (XRD) in a Philips X'Pert diffractometer using Ni-filtered Cu Kα radiation (λ = 1.5418 Å). The mechanically induced chemical reactions were considered completed when no traces of the starting reagents were observed by this technique. Impedance spectroscopy measurements were carried out on pellets (10 mm diameter and ~2 mm thickness) prepared by uniaxial pressing of the fine powders obtained by milling (sintering temperature = 1500 °C). Colloidal Pt-paint was coated on both sides of the pellets to serve as blocking electrodes. Impedance data were recorded over the 100 Hz–1 MHz frequency range as a function of temperature, by using a Solartron 1260 Frequency Response Analyzer. Sintered pellets were also examined by scanning electron microscopy in a Philips XL30 ESEM microscope equipped with an EDAX Inc. energy-dispersive X-ray detector for microanalysis.

3. Results and discussion

Depending on the Ln^{3+} cation size, rare-earth zirconates $Ln_2Zr_2O_7$ are known to exist as either pyrochlores (Ln = La to Gd) or anion deficient fluorites (Ln = Tb–Lu and Y^{3+}). In addition, some

Table 1
Compositions of all $Gd_{2-y}Ln_yZr_2O_7$ samples analyzed in this work. Ionic radii shown are taken from [16], assuming a common coordination number equal to 8 (R_{Gd} = 1.053 Å).

Ln^{3+}	*R* (Å)	Chemical formula
Er	1.004	$Gd_{2-y}Er_yZr_2O_7$ (*y* = 0.2, 0.4, 0.8)
Y	1.019	$Gd_{2-y}Y_yZr_2O_7$ (*y* = 0.2, 0.4)
Dy	1.027	$Gd_{2-y}Dy_yZr_2O_7$ (*y* = 0.2, 0.4, 0.8)
Sm	1.079	$Gd_{2-y}Sm_yZr_2O_7$ (*y* = 0.2, 0.4, 0.8)
Nd	1.109	$Gd_{2-y}Nd_yZr_2O_7$ (*y* = 0.3, 0.6, 0.8)
La	1.160	$Gd_{2-y}La_yZr_2O_7$ (*y* = 0.2, 0.3, 0.4)

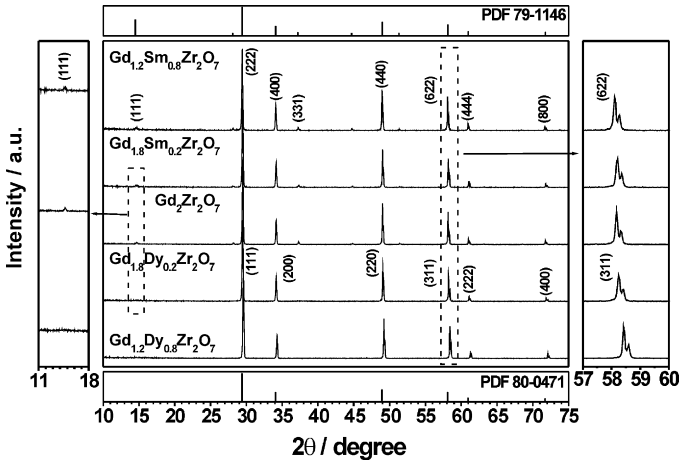

Fig. 1. XRD patterns obtained for selected Sm- or Dy-containing $Gd_{2-y}Ln_yZr_2O_7$ samples after firing at 1500 °C and slow cooling to room-temperature. Whereas the superstructure reflections characterizing the pyrochlore long-range ordering of cations and anion vacancies, are evident in the first ones (e.g. (1 1 1) or (3 3 1) at ~15° and 37° (2θ) respectively), they are absent in the latter suggesting increasing structural disorder as Gd^{3+} atoms are replaced by the smaller Dy^{3+} ions. Reported XRD patters of F- and P-type $Gd_2Zr_2O_7$ as well as that of our pristine $Gd_2Zr_2O_7$ powders are also shown as a reference. Numbers in parenthesis are the fluorite and pyrochlore Miller indexes of each reflection. Left and right inserts show an enlargement of some areas of the XRD patterns.

pyrochlore-type zirconates (Ln = Nd–Gd) disorder and become fluorites at high temperature (e.g. ~1550 °C for P-$Gd_2Zr_2O_7$). However, it has been shown that even in zirconates which are nominally fluorites such as $Y_2Zr_2O_7$ or the high temperature form of $Gd_2Zr_2O_7$, random mixing of cations and anion vacancies in their corresponding substructures is never complete [14,15]. Therefore, they shall not be considered as "true" fluorite-type materials but better represented by ordered pyrochlore-type microdomains in a disordered fluorite-type matrix.

As shown in Fig. 1, replacing Gd in P-$Gd_2Zr_2O_7$ by homovalent Ln^{3+} cations produced either anion deficient fluorites or pyrochlores. Thus, Gd substitution by smaller lanthanides such as Dy, Y or Er (R_{Gd} = 1.053 Å > R_{Dy} = 1.027 Å > R_Y = 1.019 Å > R_{Er} = 1.004 Å [16]) rendered single phase materials with XRD patterns resembling the characteristic of anion deficient fluorites. However, when Gd was replaced by larger cations such as Sm, Nd or La (R_{Sm} = 1.079 Å < R_{Nd} = 1.109 Å < R_{La} = 1.16 Å), the XRD patterns contained all the superstructure reflections characteristic of pyrochlores (e.g. the (1 1 1) and (3 3 1) reflections at ~15° and 38° (2θ) respectively). Therefore, decreasing the average size of cations at the A-site and thus the value of the R_A/R_{Zr} ratio, increases the intrinsic structural disorder of P-$Gd_2Zr_2O_7$ and induces a pyrochlore-to-fluorite phase transition. In contrast, better ordered pyrochlores are obtained when Gd^{3+} is replaced by larger lanthanides (the R_A/R_{Zr} ratio increases). It is worth mentioning that although cation size is not the only parameter of significance in determining the degree of structural ordering/disordering in pyrochlores, it is certainly the most simple and convenient for the purposes of this work.

Peak shifts towards higher ($Gd_{2-y}Dy_yZr_2O_7$) and lower ($Gd_{2-y}Sm_yZr_2O_7$) angles observed in the XRD patterns presented in Fig. 1, confirm the formation of the title solid solutions and the expected reduction or enlargement of lattice parameters when Gd is replaced by smaller (Er, Y and Dy) or larger cations (Sm, Nd and La) respectively.

As for the electrical properties, the $Gd_{2-y}Ln_yZr_2O_7$ samples gave rise to impedance spectra similar to those typical of most solid electrolyte systems. Fig. 2 shows the complex impedance plot

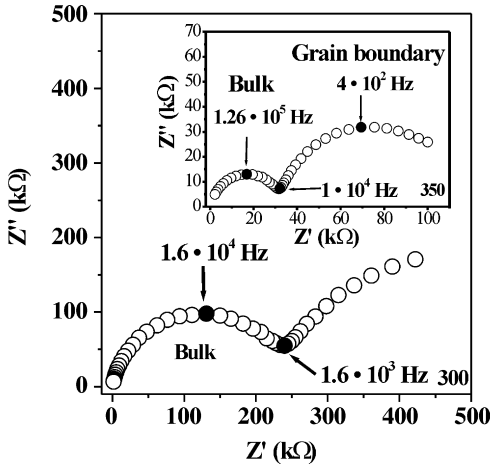

Fig. 2. Complex impedance plot obtained at 300 and 350 °C (inset) for $Gd_{1.7}Nd_{0.3}Zr_2O_7$. Solid circles represent selected frequencies in Hertzs.

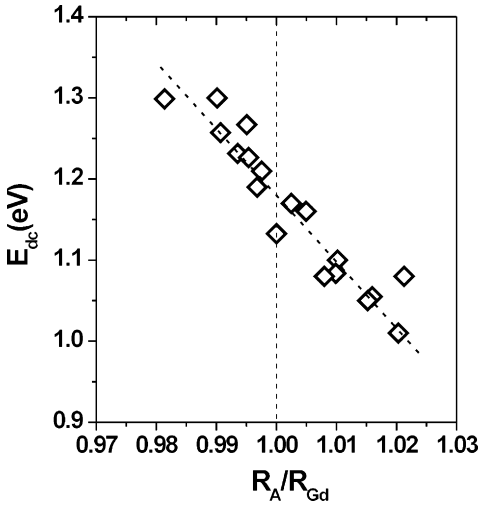

Fig. 4. dc activation energies for oxygen ion diffusion in $Gd_{2-y}Ln_yZr_2O_7$ plotted as a function of a normalized ionic radius of the A cation where $R_A/R_{Gd} = 1$ corresponds to the undoped material. The dashed line is not a linear fit and is only shown to emphasize a trend.

obtained at 300 and 350 °C (inset) for the $Gd_{1.7}Nd_{0.3}Zr_2O_7$ composition where two main features are evident, i.e. an incomplete arc at low frequencies with capacitance values typical of grain boundary contributions ($\sim 7 \times 10^{-10}$ F cm^{-1} at 350 °C) and another one at high frequencies associated with the bulk contribution ($\sim 5 \times 10^{-12}$ F cm^{-1} at both temperatures). Bulk dc conductivities for the whole series were calculated from these experimental data and their temperature dependence analyzed by using an Arrhenius-type law of the form $\sigma_{dc} = (\sigma_0/T)\,exp(-E_{dc}/kT)$, where E_{dc} is the activation energy for the conduction process and σ_0 the pre-exponential factor. Fig. 3 shows such representations for selected samples where the solid lines are least squares best fits to an Arrhenius law confirming that ion diffusion in these materials is thermally activated. The dc activation energies calculated from the slope of these plots were found to vary significantly with Gd substitution; thus, the E_{dc} value of 1.13 eV obtained for undoped P-$Gd_2Zr_2O_7$, increases to ~1.3 eV in fluorite-type $Gd_{1.2}Er_{0.8}Zr_2O_7$ or $Gd_{1.2}Dy_{0.8}Zr_2O_7$ and decreases to 1.0 eV in pyrochlore-type $Gd_{1.6}La_{0.4}Zr_2O_7$. In order to analyze the effect of the existing structural ordering/disordering on the electrical properties of P-$Gd_2Zr_2O_7$, we plotted in Fig. 4 the calculated dc

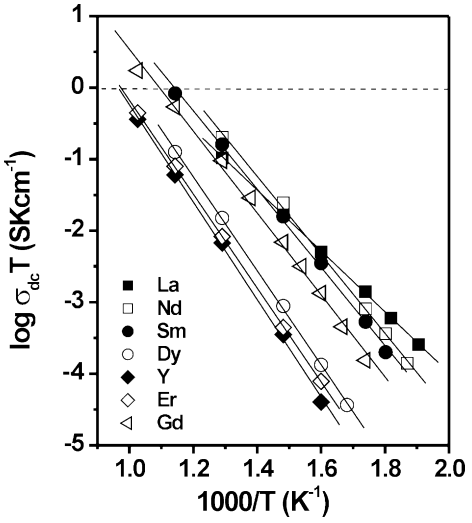

Fig. 3. Arrhenius plots of dc conductivity for selected samples: $Gd_{1.2}Ln_{0.8}Zr_2O_7$ (Ln = Er, Dy, Sm, Nd, La), $Gd_2Zr_2O_7$ and $Gd_{1.6}Y_{0.4}Zr_2O_7$. Solid lines are the least squares best linear fits to the experimental data.

activation energies for the whole series as a function of a normalized average A cation ionic radius. To calculate the average R_A size in each sample, we used the individual ionic radii given by Shannon [16] as well as the fraction of each cation present: e.g., the average R_A size in $Gd_{1.7}Nd_{0.3}Zr_2O_7$ would be calculated as follows: $R_A = [1.7R_{Gd} + 0.3R_{Nd}]/2$. To facilitate the estimation, we have assumed no mixing between cations at the A and B-sites that is, Gd^{3+} and Ln^{3+} ions are constraint to the A-site whereas Zr^{4+} is exclusively located at the B position. Finally, to ease the discussion we have also normalized the R_A value in each sample relative to that of Gd^{3+} and plotted the experimental data versus the R_A/R_{Gd} ratio.

As Fig. 4 shows, the E_{dc} needed for oxygen migration increases significantly with decreasing R_A/R_{Gd} (increasing structural disordering); in fact, the E_{dc} follows a general trend which persists even across the theoretical fluorite/pyrochlore phase boundary in the system, and shows a sharp and almost linear decrease with increasing R_A/R_{Gd}. As cell volume in fluorite and pyrochlore-type $Ln_2Zr_2O_7$ zirconates is to a good approximation, linearly dependent on the ionic radius of the A-type cation [17], Gd substitutions in P-$Gd_2Zr_2O_7$ by larger cations will increase cell volume and thus, facilitate ion hopping. Therefore, a lower energy barrier for mobile oxygen ions would be expected which is consistent with the experimental data of the title series and with those published previously in similar pyrochlore systems [18].

Fig. 5 shows the evolution of the bulk conductivity in the $Gd_{2-y}Ln_yZr_2O_7$ system versus the normalized R_A/R_{Gd} ratio at two measuring temperatures, 500 and 800 °C. As this figure shows, conductivity in the series does not depend only on the dopants size and their influence in cell volume but also in their effect on oxygen vacancies ordering. Thus, conductivity at any given temperature is higher for the pyrochlore-type materials than for those showing the anion deficient fluorite structure. Within each structural type however, conductivity values at high temperature remain almost constant and independent of the dopant cation and composition. As Fig. 6a and b shows, these changes in conductivity cannot be explained by differences in microstructure since all the samples analyzed showed after sintering, similar final porosity and grain size.

Finally, we have not observed a peak in conductivity close to the pyrochlore/fluorite phase boundary as suggested by some other works carried out in similar $Ln_2Zr_2O_7$ systems [17] although con-

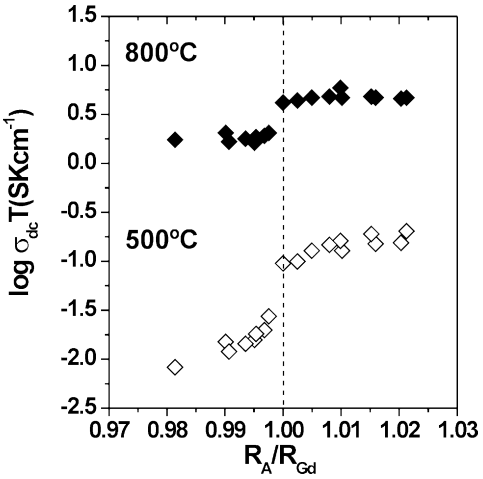

Fig. 5. The effect of homovalent Gd substitution in the bulk conductivity of the pyrochlore-type $Gd_2Zr_2O_7$, plotted as a function of a normalized averaged A cation size.

ductivity in the first is certainly higher than in the latter. Many papers have been published dealing with the effect of dopant size on the conductivity of different ionic conductors and it is generally accepted that those inducing the lowest strain in the crystal lattice of the host material, exhibit the highest conductivity. Thus, in the $(Gd_{1-x}A_x)_2Ti_2O_7$ system (with A = Mg^{2+}, Ca^{2+}, Sr^{2+}, K^+), the highest conductivity values were obtained for Ca^{2+}, which exhibits the closest size match to Gd^{3+} [19]. Similar studies carried out in fluorite-type $Ln_yCe_{1-y}O_{2-\delta}$ have also shown a minimum in the activation energy and a maximum in conductivity for Gd^{3+}, with the closest size match to Ce^{4+} [20]. In our case, the pristine material P-$Gd_2Zr_2O_7$ is not an insulator as $Gd_2Ti_2O_7$ neither doping is used to create vacancies as in CeO_2 but to manipulate the degree of structural ordering/disordering. Our results show that P-$Gd_2Zr_2O_7$ is highly tolerant to chemical substitutions at the A-site with the best dopants being those which increase the size mismatch between cations at the A and B-sites that is, lanthanide ions larger than Gd^{3+}. Decreasing number of mobile charge carriers with increasing structural ordering is apparently compensated by decreasing activation energies for migration and thus, conductivity remains almost constant (or even increases slightly) as observed in the $Gd_2(Ti_{1-y}Zr_y)_2O_7$ system when Zr^{4+} is replaced by Ti^{4+} [21,22].

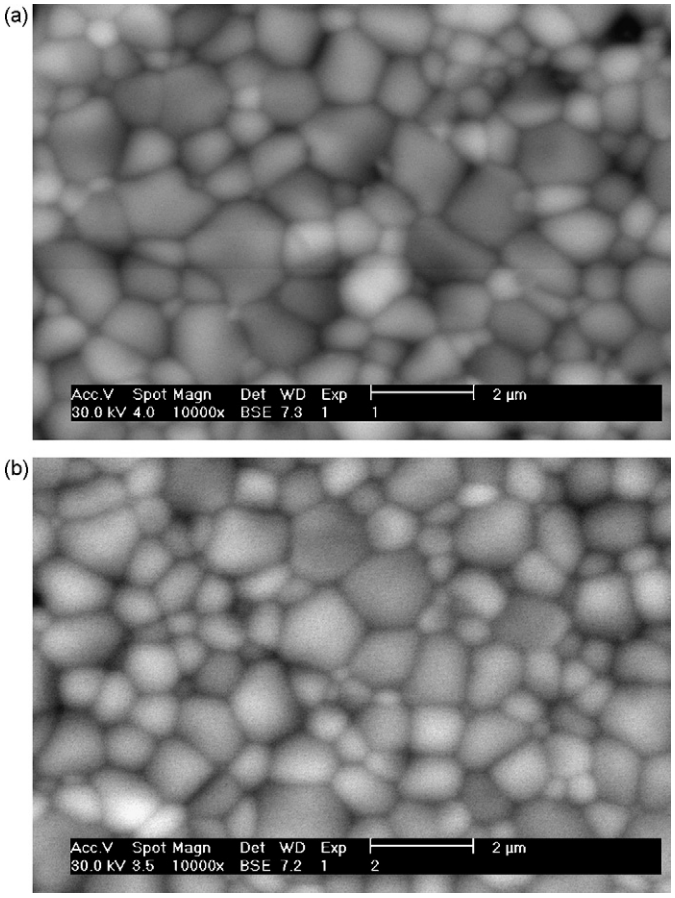

Fig. 6. Scanning electron micrographs of $Gd_2Zr_2O_7$ (a) and $Gd_{1.6}La_{0.4}Zr_2O_7$ (b), after pressing and sintering as described in Section 2.

4. Conclusion

We have shown that pyrochlore-type $Gd_2Zr_2O_7$ is highly tolerant to a large number of A-site lanthanide substitutions. Whereas replacing Gd by smaller lanthanides yields anion deficient fluorites, larger cations produce increasingly ordered pyrochlores. Interestingly, the $Gd_{2-y}Ln_yZr_2O_7$ solid solutions (Ln = Sm, Nd and La) are good ionic conductors with smaller dc activation energy for oxygen migration than that observed for the pristine P-$Gd_2Zr_2O_7$.

Acknowledgements

This work has been carried out with the financial support of Mexican Conacyt (SEP-2003-C02-44075) and Spanish MCI (MAT2008-06517-C02-02).

References

[1] B.J. Wuensch, K.W. Eberman, C. Heremans, E.M. Ku, P. Onnerud, E.M.E. Yeo, S.M. Haile, J.K. Stalick, J.D. Jorgensen, Solid State Ionics 129 (2000) 111–133.
[2] O. Porat, C. Heremans, H.L. Tuller, Solid State Ionics 94 (1997) 75–83.
[3] A.V. Shlyakhtina, I.V. Kolbanev, A.V. Knotko, M.V. Boguslavskii, S.Yu. Stefanovich, O.K. Karyagina, L.G. Shcherbakova, Inorg. Mater. 41 (2005) 854–863.
[4] M. Subramanian, G. Aravamudan, G.V. Subba Rao, Prog. Solid State Chem. 15 (1983) 55–143.
[5] M. Pirzada, R.W. Grimes, L. Minervini, J.F. Maguire, K.E. Sickafus, Solid State Ionics 140 (2001) 201–208.
[6] P.J. Wilde, C.R.A. Catlow, Solid State Ionics 112 (1998) 185–195.
[7] R.E. Williford, W.J. Weber, R. Devanathan, J.D. Gale, J. Electroceram. 3 (4) (1999) 409–424.
[8] P.J. Wilde, C.R.A. Catlow, Solid State Ionics 112 (1998) 173–183.
[9] M.P. Van Dijk, A.J. Burggraaf, A.N. Cormack, C.R.A. Catlow, Solid State Ionics 17 (1985) 159–167.
[10] J.A. Díaz-Guillén, M.R. Díaz-Guillén, J.M. Almanza, A.F. Fuentes, J. Santamaría, C. León, J. Phys. -Condes. Matter 19 (2007) 356212.
[11] J.A. Díaz-Guillén, M.R. Díaz-Guillén, K.P. Padmasree, J.M. Almanza, A.F. Fuentes, J. Santamaría, C. León, Bol. Soc. Esp. Ceram. V 47 (2008) 159–164.
[12] K.J. Moreno, R. Silva-Rodrigo, A.F. Fuentes, J. Alloys Compd. 390 (2005) 230–235.
[13] A.F. Fuentes, K. Boulahya, M. Maczka, J. Hanuza, U. Amador, Solid State Sci. 7 (2005) 343–353.
[14] N. Kim, C.P. Grey, J. Solid State Chem. 175 (2003) 110–115.
[15] T. Moriga, A. Yoshiasa, F. Kanamaru, K. Koto, M. Yoshimura, S. Somiya, Solid State Ionics 31 (1989) 319–328.
[16] R.D. Shannon, Acta Crystallogr. A 32 (1976) 751–767.
[17] H. Yamamura, H. Nishino, K. Kakinuma, K. Nomura, Solid State Ionics 158 (2003) 359–365.
[18] H. Nishino, H. Yamamura, T. Arai, K. Kakinuma, K. Nomura, J. Ceram. Soc. Japan 112 (2004) 541–546.
[19] H.L. Tuller, J. Phys. Chem. Solids 55 (1994) 1393–1404.
[20] R. Gerhardt-Anderson, A.S. Nowick, Solid State Ionics 5 (1981) 547–550.
[21] P.K. Moon, H.L. Tuller, Solid State Ionics 28–30 (1988) 470–474.
[22] K.J. Moreno, G. Mendoza-Suárez, A.F. Fuentes, J. García-Barriocanal, C. León, J. Santamaría, Phys. Rev. B 71 (2005) 132301.